Biochemical and Biophysical Research Communications 440 (2013) 283–288

Contents lists available at ScienceDirect

Biochemical and Biophysical Research Communications

journal homepage: www.elsevier.com/locate/ybbrc

Characterization of a novel mutant KCNQ1 channel subunit lacking a large part of the C-terminal domain

Katsuya Kimoto [a], Koshi Kinoshita [b], Tomoki Yokoyama [a], Yukiko Hata [b], Takuto Komatsu [a], Eikichi Tsushima [a], Kohki Nishide [a], Yoshiaki Yamaguchi [c], Koichi Mizumaki [d], Toshihide Tabata [a,*], Hiroshi Inoue [c], Naoki Nishida [b], Kenkichi Fukurotani [a]

[a] Laboratory for Neural Information Technology, Graduate School of Sciences and Engineering, University of Toyama, 3190 Gofuku, Toyama 930-8555, Japan
[b] Department of Legal Medicine, Graduate School of Medical and Pharmaceutical Sciences, University of Toyama, 2630 Sugitani, Toyama 930-0194, Japan
[c] Second Department of Internal Medicine, Graduate School of Medical and Pharmaceutical Sciences, University of Toyama, 2630 Sugitani, Toyama 930-0194, Japan
[d] Clinical Research and Ethics Center, Graduate School of Medical and Pharmaceutical Sciences, University of Toyama, 2630 Sugitani, Toyama 930-0194, Japan

ARTICLE INFO

Article history:
Received 10 September 2013
Available online 23 September 2013

Keywords:
Arrhythmia
LQT1
K_V*LQT1*
K_V*7.1*
minK
IsK

ABSTRACT

A mutation of *KCNQ1* gene encoding the alpha subunit of the channel mediating the slow delayed rectifier K^+ current in cardiomyocytes may cause severe arrhythmic disorders. We identified *KCNQ1(Y461X)*, a novel mutant gene encoding KCNQ1 subunit whose C-terminal domain is truncated at tyrosine 461 from a man with a mild QT interval prolongation. We made whole-cell voltage-clamp recordings from HEK-293T cells transfected with either of wild-type *KCNQ1* [*KCNQ1(WT)*], *KCNQ1(Y461X)*, or their mixture plus *KCNE1* auxiliary subunit gene. The *KCNQ1(Y461X)*-transfected cells showed no delayed rectifying current. The cells transfected with both *KCNQ1(WT)* and *KCNQ1(Y461X)* showed the delayed rectifying current that is thought to be mediated largely by homomeric channel consisting of KCNQ1(WT) subunit because its voltage-dependence of activation, activation rate, and deactivation rate were similar to the current in the *KCNQ1(WT)*-transfected cells. The immunoblots of HEK-293T cell-derived lysates showed that KCNQ1(Y461X) subunit cannot form channel tetramers by itself or with KCNQ1(WT) subunit. Moreover, immunocytochemical analysis in HEK-293T cells showed that the surface expression level of KCNQ1(Y461X) subunit was very low with or without KCNQ1(WT) subunit. These findings suggest that the massive loss of the C-terminal domain of KCNQ1 subunit impairs the assembly, trafficking, and function of the mutant subunit-containing channels, whereas the mutant subunit does not interfere with the functional expression of the homomeric wild-type channel. Therefore, the homozygous but not heterozygous inheritance of *KCNQ1(Y461X)* might cause major arrhythmic disorders. This study provides a new insight into the structure–function relation of KCNQ1 channel and treatments of cardiac channelopathies.

1. Introduction

KCNQ1 gene encodes the alpha subunit that associates with KCNE1 beta subunit to form the KCNQ1 channel that mediates the slow delayed rectifier K^+ current in cardiomyocytes [1,2]. This current is responsible for accelerating the repolarizing phases of action potentials and prevents premature action potential regeneration [3,4]. A mutation of *KCNQ1* may cause type-1 long QT syndrome [5], which is associated with a prolongation of QT interval in the electrocardiogram and increases risk for severe arrhythmic disorders [6].

We recently found *KCNQ1(Y461X)*, a novel mutant gene from a man with a mild QT interval prolongation. Surprisingly, the subject has not shown major cardiac disorders although the KCNQ1(Y461X) subunit lacks a large part of the C-terminal domain including the sites suggested to be crucial for the functional expression of KCNQ1 channel (see Section 4). We assessed whether and how *KCNQ1(Y461X)* affects KCNQ1 channel function in heterologous expression cells using a patch-clamp technique. Moreover, we examined the molecular behavior of KCNQ1(Y461X) subunit by immunoblotting and immunocytochemistry.

Abbreviations: *KCNQ1(WT)*, wild-type *KCNQ1*; *KCNQ1(Y461X)*, mutant *KCNQ1* producing a subunit truncated at tyrosine 461; (FLAG-)WT(+E1) cell, cell transfected with (*FLAG*-fused) *KCNQ1(WT)* (and *KCNE1*); (FLAG-)YX(+E1) cell, cell transfected with (*FLAG*-fused) *KCNQ1(Y461X)* and (and *KCNE1*); (FLAG-)YX/WT(+E1) cell, cell transfected with (*FLAG*-fused) *KCNQ1(WT) and KCNQ1(461X)* (plus *KCNE1*).

* Corresponding author. Fax: +81 76 445 6703.
E-mail address: ttabata@eng.u-toyama.ac.jp (T. Tabata).

0006-291X/$ - see front matter © 2013 Elsevier Inc. All rights reserved.
http://dx.doi.org/10.1016/j.bbrc.2013.09.075

2. Materials and methods

2.1. Genetic analysis

The diagnosis of and peripheral blood sampling from the subject were performed at the Second Department of Internal Medicine, Toyama University Hospital under the approval of the university's committee on utilization of human genes (#22–9). The written informed consent was obtained from the subjects before blood sampling. Amplification and sequencing of *KCNQ1* exons 1–16 from the genomic DNA were performed as described elsewhere [7].

The amino acid sequences of KCNQ1 homologs were compared using GENETYX software (GENETYX, Tokyo, Japan).

2.2. Plasmid construction

pReceiver-M12 plasmid vector encoding 3xFLAG-fused KCNQ1(WT) subunit [FLAG-*KCNQ1(WT)*] was purchased from GeneCopoeia (Rockville, MD, USA). FLAG-*KCNQ1(Y461X)* was generated by site-directed mutagenesis on FLAG-*KCNQ1(WT)*. pCAGGS-*KCNQ1(WT)* and pCAGGS-*KCNQ1(Y461X)* encoding epitope-free KCNQ1 subunits were constructed by inserting cDNA's amplified from sites between the *EcoR* I and *Sma* I sites of FLAG-*KCNQ1(WT)* and FLAG-*KCNQ1(Y461X)* into the blunt-ended *Xho* I sites of pCAGGS plasmid vector, respectively. *KCNE1* cDNA was cloned from the genomic DNA, amplified using the primers flanked by *EcoR* I and *Sma* I sites, and inserted into pReceiver-M12 vector pre-digested at the *EcoR* I and *Sma* I sites (FLAG-*KCNE1*). HA-*KCNE1* was constructed by replacing the 3xFLAG sequence of FLAG-*KCNE1* with a 2xHA sequence.

2.3. Cell preparation

For electrophysiological analysis, HEK-293T cells were cultured in 10% fetal bovine serum-supplemented Dulbecco's modified Eagle medium (11995-065, Life Technologies) at 37 °C in 5% CO_2. Three days before the measurements, the cells were transferred to 35-mm dishes (353001, BD, Franklin Lakes, NJ, USA). Two days before the measurements, the cells were transfected with enhanced green fluorescent protein (EGFP) gene-containing pCAGGS plasmid vector (25 ng/dish), FLAG-*KCNE1* (150 ng/dish), and either of pCAGGS-*KCNQ1(WT)* (75 ng/dish), pCAGGS-*KCNQ1(Y461X)* (75 ng/dish), or a mixture of pCAGGS-*KCNQ1(WT)* and pCAGGS-*KCNQ1(Y461X)* (37.5 ng/dish each) (WT+E1, YX+E1, and YX/WT+E1 cells, respectively) using TransIT-293 reagent (Mirus Bio, Madison, WI, USA).

For immunoblot analysis, HEK-293T cells were cultured on 60-mm plastic dishes (150288, Thermo Fisher Scientific, Waltham, MA, USA). Two days before harvesting, the cells were transfected with either of FLAG-*KCNQ1(WT)* (750 ng/dish), FLAG-*KCNQ1(Y461X)* (750 ng/dish), or a mixture of pCAGGS-*KCNQ1(WT)* and FLAG-*KCNQ1(Y461X)* (375 ng/dish each) using TransIT-293 reagent.

For immunocytochemistry, HEK-293T cells were cultured on 35-mm glass-based dishes (D111300, Matsunami, Osaka, Japan). Two days before immunostaining, the cells were transfected with HA-*KCNE1* (125 ng/dish) and either of pCAGGS-*KCNQ1(WT)* (125 ng/dish), FLAG-*KCNQ1(Y461X)* (125 ng/dish), or a mixture of pCAGGS-*KCNQ1(WT)* and FLAG-*KCNQ1(Y461X)* (62.5 ng/dish each) using TransIT-293 reagent.

2.4. Electrophysiological analysis

Rupture-patch whole-cell voltage-clamp recordings were made from the EGFP-positive cells. A glass recording pipette (tip resistance, 3–5 MΩ) was filled with a solution containing (in mM) 134 potassium D-gluconic acid, 7.6 KCl, 9 KOH, 10 NaCl, 1.2 $MgCl_2$, 10 HEPES, 0.5 EGTA, and 4 adenosine triphosphate magnesium salt (pH, adjusted to 7.3 with KOH). The culture dish was perfused at a rate of 1.2 ml/min with a pre-warmed (36–38 °C) solution containing (in mM) 147 NaCl, 4 KCl, 2 $CaCl_2$, 1 $MgCl_2$, 10 HEPES, and 10 D-glucose (pH, adjusted to 7.4 with NaOH). The command voltages were corrected for a liquid junction potential between the pipette and bath solutions. Current signals were acquired with an EPC 8 amplifier (HEKA, Lambrecht-Pfalz, Germany) controlled by Patchmaster software (version, 2x35; HEKA). The holding potential was −80 mV. After membrane rupture, the pipette capacitance was canceled electronically and then, responses to 10 sets of bipolar voltage pulses (−75 mV, 40 ms and −85 mV, 40 ms) were recorded at a cut-off frequency of 30 kHz and a sampling rate of 50 kHz. Then, the main component of the membrane capacitance was cancelled electronically and responses to test stimuli were recorded with 60% electronic series resistance compensation and at a cut-off frequency of 300 Hz and a sampling rate of 1 kHz.

The amplitude of linear leakage and the membrane capacitance were estimated from the average of the bipolar pulse-evoked responses. The text and graphs report current densities after subtraction of the linear leakages while the traces show raw data including the linear leakages.

To quantify the voltage-dependence of activation extent of KCNQ1 channel current, a Boltzmann equation [$I_{tail} = \frac{A}{1+exp\left[\frac{V_{half} - V_{first}}{K}\right]}$, where I_{tail}, A, V_{half}, V_{first}, and K are the peak amplitude of a tail current, scale factor, voltage for half-maximal activation, first-step voltage, and slope, respectively] was fitted to the *I–V* relation of each cell using IGOR Pro software (versions, 6.22A and 6.32A; WaveMetrics, Lake Oswego, OR, USA). To quantify the activation and deactivation rates, single- and double-exponential functions were fitted to the rise (270–700 ms of a depolarizing step onset) and decay (4–3999 ms of the depolarizing step offset) of the KCNQ1 channel-mediated current, respectively using IGOR Pro software. Numerical data groups are expressed as mean ± SEM throughout the text and figures. A difference in current density between a pair of the data groups was examined using Wilcoxon rank sum test because some data groups had non-normal distributions. A difference in kinetic parameters was examined using unpaired *t*-test because most data groups had normal distributions.

2.5. Immunoblot analysis

The transfected HEK-293T cells were washed twice with chilled Dulbecco's phosphate-buffered saline (DPBS). The cells were scraped in 1.5 ml of DPBS and then spun down at 1000 rpm for 5 min. The collected cells were lysed with 300 μl of a buffer consisting of 150 mM NaCl, 20 mM Tris–HCl (pH, 7.5), 1% Triton X-100, 0.5 mM ethylenediaminetetraacetic acid, and 10 μl/ml protease inhibitor mix (80-6501-23, GE Healthcare, Little Chalfont, UK) and incubated on ice for 1 h. The lysate was centrifuged at 15,000 rpm and 4 °C for 20 min and then the supernatant was transferred to a new tube. The supernatant was incubated with a 2x sodium dodecyl sulfate (SDS) sample buffer consisting of 0.5% SDS, 100 mM Tris (pH, 6.8), 20% glycerol, and 200 mM dithiothreitol at room temperature (RT) for 30 min. Electrophoresis was performed at a constant voltage of 120 V for 1 h. The materials on the gel were transferred to a reactivated polyvinyldene fluoride membrane (Hybond-P, RPN303F, GE Healthcare) containing a buffer consisting of 0.1% SDS, 25 mM Tris–HCl (pH, 8.3), 192 mM glycine, 5% methanol. The blotted membrane was consecutively rinsed with a Tris-buffered saline (TBS) consisting of 20 mM Tris–HCl (pH7.6) and 137 mM NaCl, blocked by TBS containing 9% skim milk and 0.05% Tween20 (161-0781, Bio-Rad Laboratories, Hercules, CA,

USA) at RT for 2 h, incubated with TBS containing a mouse monoclonal horse radish peroxidase (HRP)-conjugated anti-FLAG antibody (M185-7, Medical & Biological Laboratories, Nagoya, Aichi, Japan; dilution, 1:4000), 1% skim milk, and 0.05% Tween20 at RT for 1 h, and washed three times with TBS containing 0.05% Tween20 (10 min for each time). The membrane was treated with ECL Prime reagents (RPN2232, GE Healthcare). Immunofluorescent signals were detected using a LAS-4000 camera system (Fujifilm, Tokyo, Japan).

2.6. Immunocytochemistry

All the following reagents were prepared as DPBS solutions. The cells were consecutively rinsed twice with DPBS (37 °C), fixed with 4% paraformaldehyde (RT, 15 min), rinsed three times with DPBS (RT), treated with 0.1% Triton X-100 plus 5% bovine serum albumin (BSA; A7906, Sigma–Aldrich, St. Louis, MO, USA) (RT, 30 min), and rinsed three times with DPBS. For detecting an immunoreactivity for KCNQ1(WT) subunit, the cells were consecutively incubated with a rabbit anti-KCNQ1 antibody (sc-20816, Santa Cruz Biotechnology, Santa Cruz, CA, USA; dilution, 1:100) plus 1% BSA (4 °C, overnight), incubated with an Alexa Fluor 647-conjugated goat anti-rabbit IgG(H + L) antibody (A21245, Life Technologies; dilution, 1:250) plus 1% BSA (37 °C, 1 h), and rinsed three times with DPBS. For detecting an immunoreactivity for KCNQ1(Y461X) subunit, the cells were consecutively incubated with a mouse monoclonal anti-DDDDK-tag-Alexa Fluor 488 antibody (M185-A48, Medical & Biological Laboratories, Nagoya, Aichi, Japan; dilution, 1:1000) plus 1% BSA (4 °C, overnight or RT, 1 h) and rinsed three times with DPBS.

For moderately stained cells, single image slices of 488 and/or 633 nm laser beam (power, 30%)-excited immunofluorescence were captured using a TCS-SP5 confocal microscope (Leica Microsystems, Wetzlar, Germany; objective lens, oil-immersion, x63; pinhole, airy 1; gain, 650 V for 494–564 nm and 643–725 nm).

3. Results

3.1. Genetic analysis

We identified *KCNQ1(Y461X)* from a 40 years-old man. Although he has not yet shown major cardiac disorders, he displayed a mildly prolonged corrected QT interval (QTc) of 441 ms (Fig. 1A). He carries *KCNQ1(Y461X)* heterozygously.

In *KCNQ1(Y461X)*, the codon encoding Y461 was mutated to a stop codon by an insertion of A to nucleotide position 1383 (Fig. 1B). This mutation results in the truncation of a large part of the C-terminal domain of KCNQ1 subunit (Fig. 1C). Among mammalian homologs, the species of the amino acid corresponding to Y461 of human KCNQ1 subunit are not well conserved (Fig. 1D).

The subject also homozygously carries the minor variant of the serine 38/glycine 38 polymorphism of *KCNE1* [*KCNE1(38S)*] [8]. He has no mutations in the other major arrhythmia-related ion channel genes (*KCNH2, KCNE2*, or *SCN5A*; data not illustrated).

3.2. Electrophysiological analysis

To analyze the functional characteristics of KCNQ1(Y461X) subunit, we compared currents in the WT+E1, YX+E1, and YX/WT+E1 cells under voltage clamp. We applied a double-voltage-step stimulus consisting of the first step with a varying V_{first} and the second step with a fixed voltage of −50 mV to the examined cell (Fig. 2A). The WT+E1 cells showed a large slowly activating current without obvious inactivation at the first voltage step (Fig. 2B). This slowly activating current is thought to be mediated by KCNQ1 channel because such a current is not observed in non-channel gene-transfected HEK-293T cells [7,9]. The YX+E1 cells showed only a small rapidly activating current that is thought to be mediated by HEK-293T cell's native channel [7,9] (Fig. 2B).

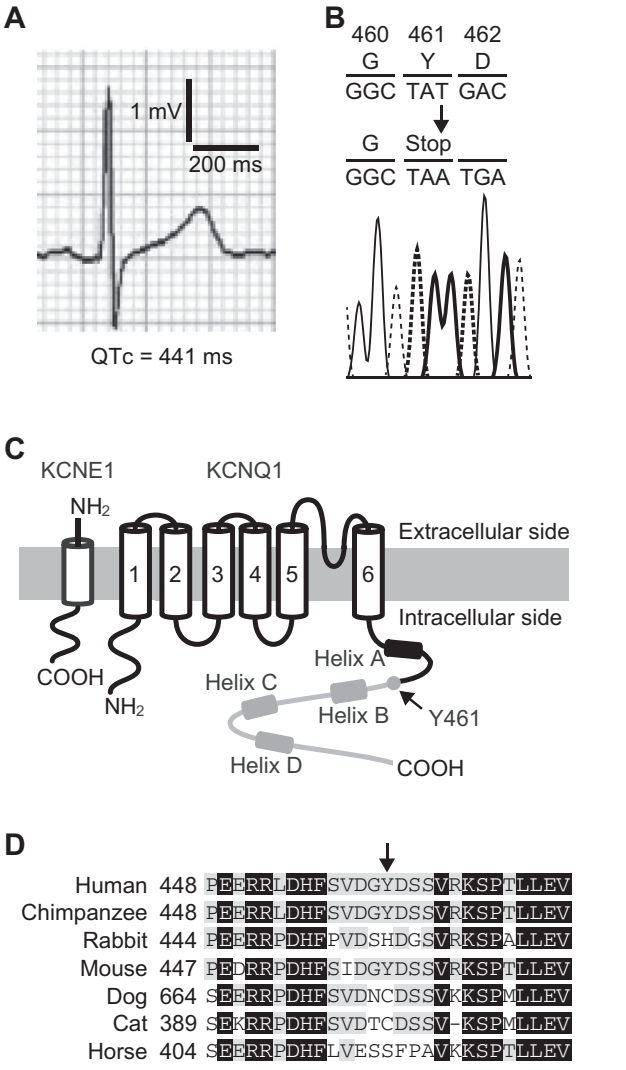

Fig. 1. *KCNQ1(Y461X)* gene and KCNQ1(Y461X) subunit. (A) Sample ECG of the male subject from whom *KCNQ1(Y461X)* was identified. (B) Comparison of the partial amino acid and DNA sequences of *KCNQ1(WT)* (upper) and *KCNQ1(Y461X)* (middle). Chromatogram (lower) indicates the sequencing data. (C) Schematic drawings of the alpha and beta subunits of KCNQ1 channel. KCNQ1(Y461X) subunit is truncated at position 461 (arrow). (D) Partial amino acid sequences of mammalian *KCNQ1* homologs aligned at the position corresponding to tyrosine 461 of human *KCNQ1* (arrow). Number, the position of the first amino acid of each partial sequence. Gray and black boxes, amino acid species conserved among some or all of the homologs, respectively.

The slowly activating current in the WT+E1 cells decayed with a I_{tail} at the second voltage step (Fig. 2B). We used the peak density of the I_{tail} to quantify the activation extent of KCNQ1 channel (Fig. 2C). The I_{tail} does not include the native channel current because the native channel current decays instantaneously upon the end of the first voltage step [7,9]. The I_{tail} density-V_{first} plot indicates that in the WT+E1 cells, the KCNQ1(WT) channel current was activated with V_{first}'s of −30 mV or above, and the activation extent was nearly saturated with V_{first}'s of + 30 mV and above. In the YX+E1 cells, KCNQ1(Y461X) channel current was not activated with all the tested V_{first}'s. The I_{tail} density with a V_{first} of +30 mV was 1.9 ± 1.1 pA/pF (n = 8) in the YX+E1 cells and 166.4 ± 27.1

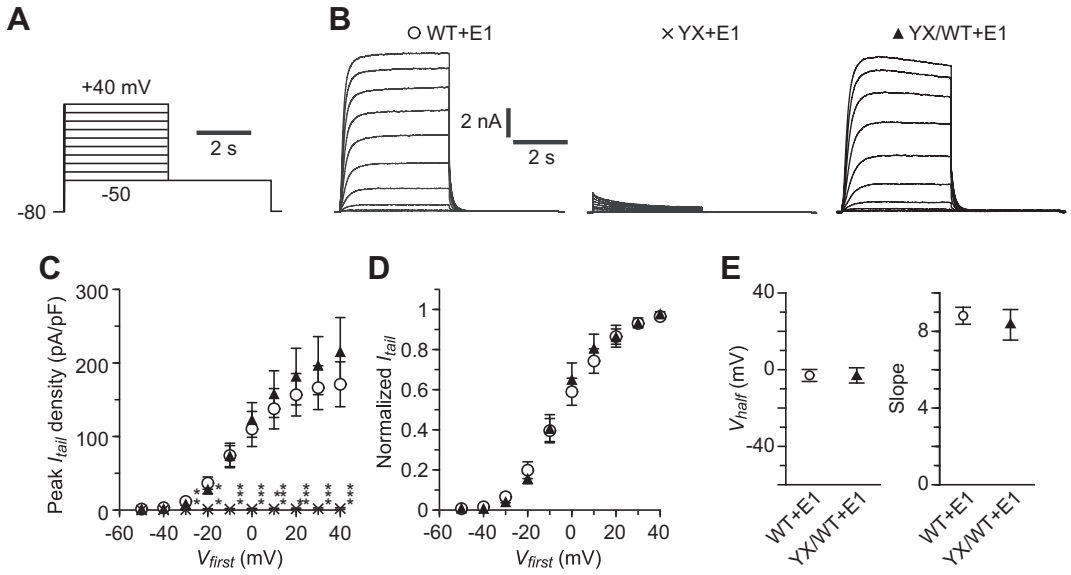

Fig. 2. Functional expression and voltage-dependence of slowly activating currents in cells transfected with *KCNQ1(WT)*, *KCNQ1(Y461X)*, or both genes. (A) Voltage stimuli used to activate KCNQ1 channels. (B) Sample current records from single cells. (C) Mean absolute peak densities of the I_{tail} as functions of the V_{first}. *, **, and ***; $p < 0.05$, $p < 0.01$, and $p < 0.001$ vs. the WT+E1 cells, Wilcoxon rank sum test. Error bars, ±SEM. The data were taken from 17 WT, 8 YX, and 8–11 YX/WT+E1 cells. (D) Mean normalized I_{tail}–V_{first} plots. I_{tail} at each V_{first} was normalized by the maximum for each cell. Error bars, ±SEM. The data were taken from the same WT+E1 and YX/WT+E1 cells as in panel C. (E) Mean V_{half} and slope estimated from the Boltzman functions fitted to the I_{tail}–V_{first} of the individual cells. Error bars, ±SEM. The data were taken from 17 WT+E1 and 11 YX/WT+E1 cells.

pA/pF ($n = 17$) in the WT+E1 cells. The I_{tail} density significantly differed between these cell groups at all the tested V_{first}'s ($p < 0.0001$–0.0455; Z −3.93 to −2.01; Wilcoxon rank sum test) except −40 mV ($p = 0.0568$, $Z = -1.90$) (Fig. 2C).

The YX/WT+E1 cells showed a slowly activating current, which was similar to that seen in the WT+E1 cells (Fig. 2B). The peak I_{tail} density of the YX/WT+E1 cells with a V_{first} of +30 mV was 196.3 ± 39.5 pA/pF ($n = 10$) (Fig. 2C). The peak I_{tail} density did not differ between the YX/WT+E1 cells and WT+E1 cells for all the tested V_{first}'s (p 0.371–0.963; Z −0.894 to 0.845; Wilcoxon rank sum test; Fig. 2C). The normalized I_{tail} density-V_{first} plot of the YX/WT+E1 cells was indistinguishable from that of the WT+E1 cells (Fig. 2D). The V_{half} and slope of the I_{tail} density-V_{first} plot of YX/WT+E1 cells (−2.98 ± 3.97 mV and 8.32 ± 0.80 respectively; $n = 11$) were not different from those of the WT+E1 cells (−3.04 ± 3.09 mV and 8.82 ± 0.44, respectively; $n = 17$) ($p = 0.990$, $t_{26} = 0.0123$ and $p = 0.555$, $t_{26} = -0.598$, respectively; unpaired t-test; Fig. 2E).

We compared the activation and deactivation rates of the slowly activating currents in the WT+E1 and YX/WT+E1 cells by fitting exponential functions to the rise and decay (i.e., I_{tail}) of the currents (Fig. 3A). The rise and decay were well described by single- and double-exponential functions, respectively (Fig. 3A, lower traces). With a V_{first} of +30 mV, the time-constant of the function fitted to the rise of the YX/WT+E1 cells (189.3 ± 16.7 ms, $n = 10$) was not different from that of the WT+E1 cells (212.8 ± 32.6 ms, $n = 16$) ($p = 0.595$, $t_{24} = -0.540$, unpaired t-test; Fig. 3B). The time-constants of the fast and slow components of the function fitted to the decay of the YX/WT+E1 cells (72.6 ± 5.6 ms and 213.0 ± 12.1 ms, respectively; $n = 10$) were not differ from those of the WT+E1 cells (69.0 ± 4.4 ms and 211.0 ± 36.8 ms, respectively; $n = 16$) ($p = 0.619$, $t_{24} = 0.503$ and $p = 0.967$, $t_{24} = 0.0417$, respectively; unpaired t-test; Fig. 3B).

3.3. Immunoblot analysis

We compared the abilities of polymerization of KCNQ1(WT) and KCNQ1(Y461X) subunits by immunoblotting the whole-cell lysates of HEK-293T cells. The target subunit was fused with FLAG and recognized with the anti-FLAG antibody. In the FLAG-WT cell lysate, bands presumably corresponding to KCNQ1(WT) subunit monomer, dimer, trimer, and tetramer were detected (Fig. 4A, 1st lane from left, arrows). In the FLAG-YX cell lysate, bands presumably corresponding to KCNQ1(Y461X) subunit monomer and dimer were found (Fig. 4A, 2nd lane, arrow heads), whereas their densities were low as compared with the KCNQ1(WT) subunit monomer and dimer bands in the FLAG-WT cell lysate. Bands corresponding to the higher polymers were not obvious. In the FLAG-YX/WT cell lysate, bands presumably corresponding to KCNQ1(Y461X) subunit monomer and dimer were detected (Fig. 4A, 3rd lane). The bands in the lysates of the transfected cells were not artifacts because they were not seen in the lysate of non-transfected cells (Fig. 4A, 4th lane). The same results were obtained in another set of immunoblot.

3.4. Immunocytochemical analysis

We compared the subcellular distributions of KCNQ1(WT) and KCNQ1(Y461X) subunits in HEK-293T cells by immunocytochemistry. KCNQ1(WT) subunit was recognized with the antibody against the C-terminal domain. KCNQ1(Y461X) subunit was fused with FLAG and recognized with the anti-FLAG antibody. In the WT+E1 cells, an immunoreactivity for KCNQ1(WT) subunit was concentrated on the plasma membrane (Fig. 4B). In the FLAG-YX+E1 cells, an immunoreactivity for KCNQ1(Y461X) subunit was concentrated in the cytoplasm (Fig. 4B). In the FLAG-YX/WT+E1 cells, immunoreactivities for KCNQ1(WT) and KCNQ1(Y461X) subunits were concentrated on the plasma membrane and in the cytoplasm, respectively (Fig. 4B).

4. Discussion

The YX+E1 cells did not display a slowly activating current (Fig. 2B and C). The FLAG-YX cells did not express a detectable amount of KCNQ1(Y461X) tetramer (Fig. 4A). The YX+E1 cells showed only a faint KCNQ1(Y461X) subunit-immunoreactivity on

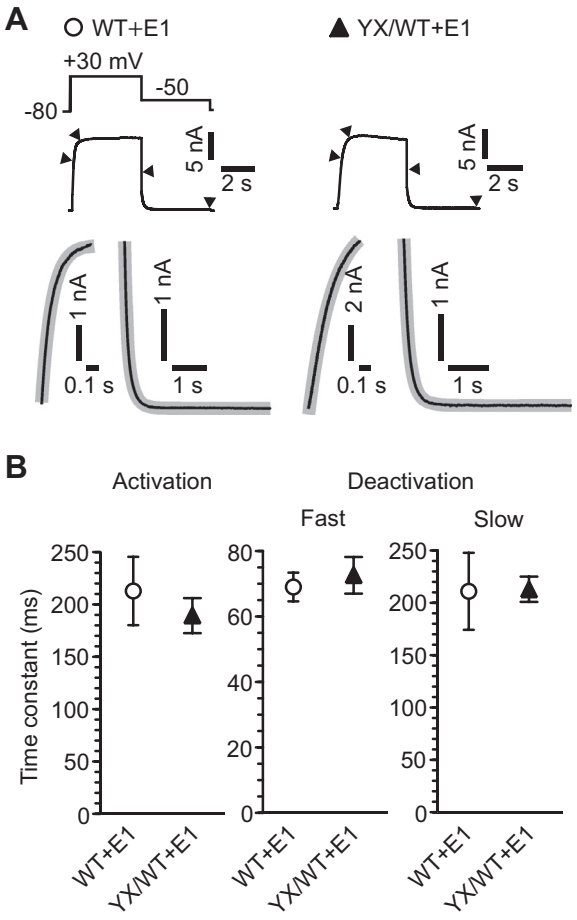

Fig. 3. Activation and deactivation rates of the slowly activating currents. (A) Rise and decay (I_{tail}) of the current evoked by a double-step voltage stimulus (schematic) were well described by single- and double-exponential functions, respectively. Upper traces, sample traces obtained from single cells. Lower traces, close-ups of the rises and decay (portions between arrow heads in the upper traces). Gray thick line, fitted functions. (B) Mean time-constants of the exponential functions fitted as shown in panel A. For deactivation, the time-constants of the fast and slow components are indicated. Error bars, ±SEM. The data were taken from 16 WT+E1 and 10 YX/WT+E1 cells.

the plasma membrane (Fig. 4B).These results suggest that KCNQ1(Y461X) subunit cannot form a significant amount of homomeric channel tetramer and that this channel is not efficiently trafficked to the cell surface.

The species of the amino acid corresponding to Y461 of human KCNQ1 is not well conserved among the mammalian homologs (Fig. 1D), indicating that the above impairments of KCNQ1(Y461X) subunit is not due to the change of the particular amino acid. Rather, the impairments may result from the lack of a large part of the C-terminal domain including helices B–D (Fig. 1C) [10,11]. It is suggested that helices A and B together accommodate one molecule of calmodulin [12], and this is important for subunit folding and channel assembly and gating [12,13]. Helices C and D may form coiled-coil structures and are thought to be important for KCNQ1 subunit polymerization [14] and interaction with KCNE1 subunit [11]. Association of KCNE1 subunit is necessary for maintaining the normal conductance and kinetics of KCNQ1 channel [1,2]. Helices C and D are also important for channel trafficking [14] and the processing of KCNQ1 protein that facilitates the cell surface expression of KCNQ1 channel [15], respectively. These molecular interactions and reactions may not occur for KCNQ1(Y461X) subunit.

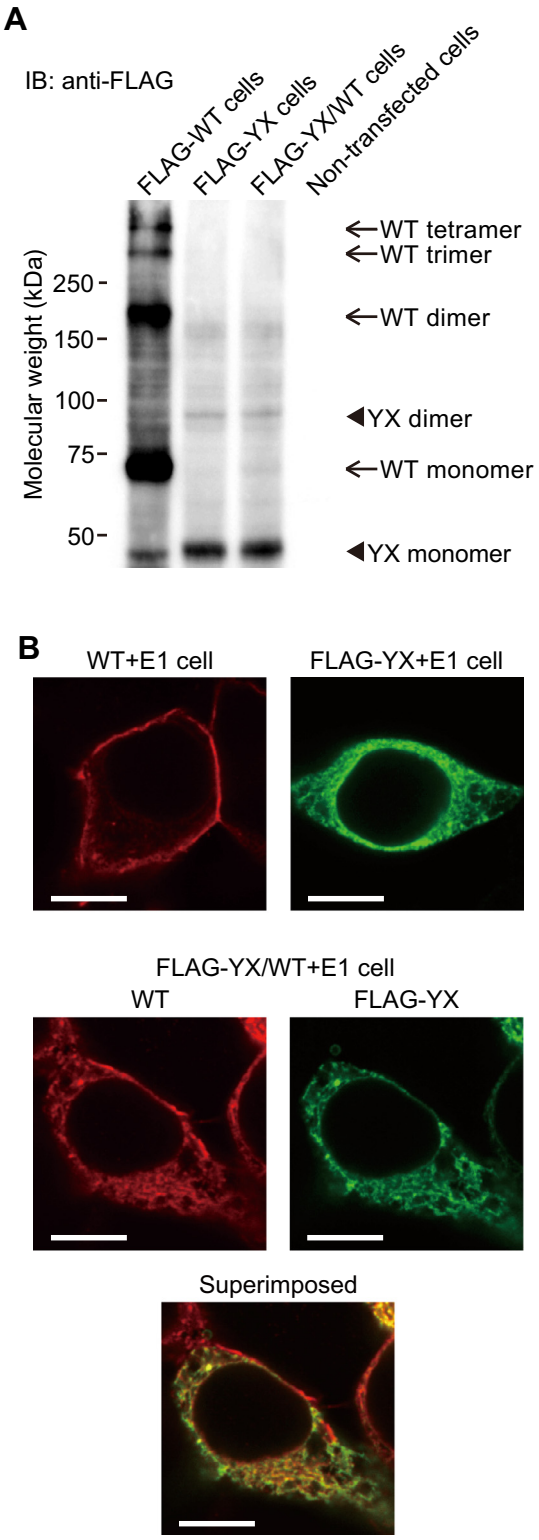

Fig. 4. Polymerization and subcellular distribution of KCNQ1(WT) and KCNQ1(Y461X) subunits. (A) Immunoblot of the whole-cell lysates of HEK-293T cells transfected with the labeled genes. Rightmost lane, negative control with the lysate of non-transfected cells. (B) Confocal images of HEK-293T cells transfected with the labeled genes. KCNQ1(WT) subunit (red) and KCNQ1(Y461X) subunit (green) were recognized with an antibody against the C-terminus of KCNQ1 subunit and an anti-FLAG antibody, respectively. For the FLAG-YX/WT+E1 cell, both KCNQ1(WT)- and FLAG-fused KCNQ1(Y461X)-immunoreactivities were shown. Calibration bars, 10 μm.

The YX/WT+E1 cells showed a slowly activating current whose voltage- and time-dependences were indistinguishable

from those in the WT+E1 cells (Figs. 2D,E and 3B). These results raise two theoretical possibilities. One is that KCNQ1(Y461X) and KCNQ1(WT) subunits cannot form functional heteromeric channels, and homomeric KCNQ1(WT) channel mediates all of the slowly activating current seen in the YX/WT+E1 cells. The other is that KCNQ1(Y461X) and KCNQ1(WT) subunits can form function heteromeric channels whose gating properties are very similar to homomeric KCNQ1(WT) channel, and the heteromeric channels and homomeric KCNQ1(WT) channel together mediate the current. The immunoblot and immunocytochemical analyses support the former. The FLAG-YX/WT cells did not express detectable amounts of KCNQ1(Y461X) subunit-containing tetramers (Fig. 4A). A negligible KCNQ1(Y461X) subunit-immunoreactivity on the plasma membrane of the FLAG-YX/WT cells (Fig. 4B) suggests that KCNQ1(WT) subunit co-expression does not rescue the trafficking of KCNQ1(Y461X) subunit-containing channels.

The density of the slowly activating current was not different between the YX/WT+E1 and WT+E1 cells (Fig. 2C) despite a difference in the amount of transfected *KCNQ1(WT)*. Such a non-proportional gene amount-current density relation was reported for *human ether-à-go-go-related gene* channel in HEK-293T cells [9]. Both non-proportional and proportional relations were reported for KCNQ1(WT) channel in non-human heterologous expression cells (e.g., Refs. [16,17]). Further studies are required to examine which cell type has the expression environment closer to that of human cardiomyocytes. However, our results (Figs. 2C and 4) suggest that KCNQ1(Y461X) subunit does not exert a strong dominant-negative effect on KCNQ1(WT) subunit. This notion is consistent with that the heterozygous *KCNQ1(Y461)* carrier has not shown major cardiac disorders. In addition, his mild QT interval prolongation could be due partly to the inheritance of the polymorphismic variant *KCNE1(38S)* [18–20].

These findings demonstrate that the massive truncation of the C-terminal domain of KCNQ1 subunit severely impairs channel assembly, trafficking, and function. The homozygous inheritance of *KCNQ1(Y461X)* might cause arrhythmic disorders due to the total loss of the cardiac slow delayed rectifier K^+ current. However, the mutant subunit does not interfere with the functional expression of homomeric wild-type channel in a dominant-negative manner. The heterozygous inheritance of *KCNQ1(Y461X)* may not cause severe arrhythmic disorders.

Acknowledgments

We thank the subject for his kind cooperation. This work was supported by a grant from First Bank of Toyama Foundation (Toyama, Japan) and partly by a grant from the Ministry of Education, Culture, Sports, Science and Technology, Japan (KAKENHI 23500384).

References

[1] J. Barhanin, F. Lesage, E. Guillemare, M. Fink, M. Lazdunski, G. Romey, K_VLQT1 and IsK (minK) proteins associate to form the I_{Ks} cardiac potassium current, Nature 384 (1996) 78–80.
[2] M.C. Sanguinetti, M.E. Curran, A. Zou, J. Shen, P.S. Spector, D.L. Atkinson, M.T. Keating, Coassembly of K_VLQT1 and minK (IsK) proteins to form cardiac I_{Ks} potassium channel, Nature 384 (1996) 80–83.
[3] M.C. Sanguinetti, N.K. Jurkiewicz, Two components of cardiac delayed rectifier K^+ current. Differential sensitivity to block by class III antiarrhythmic agents, J. Gen. Physiol. 96 (1990) 195–215.
[4] M.C. Sanguinetti, N.K. Jurkiewicz, Delayed rectifier outward K^+ current is composed of two currents in guinea pig atrial cells, Am. J. Physiol. 260 (1991) H393–399.
[5] N.J. Bokil, J.M. Baisden, D.J. Radford, K.M. Summers, Molecular genetics of long QT syndrome, Mol. Genet. Metab. 101 (2010) 1–8.
[6] S. Viskin, Long QT syndromes and torsade de pointes, Lancet 354 (1999) 1625–1633.
[7] K. Kinoshita, Y. Yamaguchi, K. Nishide, K. Kimoto, Y. Nonobe, A. Fujita, K. Asano, T. Tabata, H. Mori, H. Inoue, Y. Hata, K. Fukurotani, N. Nishida, A novel missense mutation causing a G487R substitution in the S2–S3 loop of human ether-à-go-go-related gene channel, J. Cardiovasc. Electrophysiol. 23 (2012) 1246–1253.
[8] M.J. Ackerman, D.J. Tester, G.S. Jones, M.L. Will, C.R. Burrow, M.E. Curran, Ethnic differences in cardiac potassium channel variants: implications for genetic susceptibility to sudden cardiac death and genetic testing for congenital long QT syndrome, Mayo Clin. Proc. 78 (2003) 1479–1487.
[9] Y. Hata, H. Mori, A. Tanaka, Y. Fujita, T. Shimomura, T. Tabata, K. Kinoshita, Y. Yamaguchi, F. Ichida, Y. Kominato, N. Ikeda, N. Nishida, Identification and characterization of a novel genetic mutation with prolonged QT syndrome in an unexplained postoperative death, Int. J. Legal Med. (2013), http://dx.doi.org/10.1007/s00414-013-0853-4 (in press).
[10] F.S. Choveau, M.S. Shapiro, Regions of KCNQ K^+ channels controlling functional expression, Front. Physiol. 3 (2012).
[11] Y. Haitin, B. Attali, The C-terminus of Kv7 channels: a multifunctional module, J. Physiol. 586 (2008) 1803–1810.
[12] S. Ghosh, D.A. Nunziato, G.S. Pitt, KCNQ1 assembly and function is blocked by long-QT syndrome mutations that disrupt interaction with calmodulin, Circ. Res. 98 (2006) 1048–1054.
[13] L. Shamgar, L. Ma, N. Schmitt, Y. Haitin, A. Peretz, R. Wiener, J. Hirsch, O. Pongs, B. Attali, Calmodulin is essential for cardiac I_{KS} channel gating and assembly: impaired function in long-QT mutations, Circ. Res. 98 (2006) 1055–1063.
[14] R. Wiener, Y. Haitin, L. Shamgar, M.C. Fernández-Alonso, A. Martos, O. Chomsky-Hecht, G. Rivas, B. Attali, J.A. Hirsch, The KCNQ1 (Kv7.1) COOH terminus, a multitiered scaffold for subunit assembly and protein interaction, J. Biol. Chem. 283 (2008) 5815–5830.
[15] H. Kanki, S. Kupershmidt, T. Yang, S. Wells, D.M. Roden, A structural requirement for processing the cardiac K^+ channel KCNQ1, J. Biol. Chem. 279 (2004) 33976–33983.
[16] M. Grunnet, E.R. Behr, K. Calloe, J. Hofman-Bang, J. Till, M. Christiansen, W.J. McKenna, S.P. Olesen, N. Schmitt, Functional assessment of compound mutations in the *KCNQ1* and *KCNH2* genes associated with long QT syndrome, Heart Rhythm 2 (2005) 1238–1249.
[17] J. Heijman, R.L. Spatjens, S.R. Seyen, V. Lentink, H.J. Kuijpers, I.R. Boulet, L.J. de Windt, M. David, P.G. Volders, Dominant-negative control of cAMP-dependent I_{Ks} upregulation in human long-QT syndrome type 1, Circ. Res. 110 (2012) 211–219.
[18] T.V. McDonald, Z. Yu, Z. Ming, E. Palma, M.B. Meyers, K.W. Wang, S.A. Goldstein, G.I. Fishman, A minK-HERG complex regulates the cardiac potassium current I_{Kr}, Nature 388 (1997) 289–292.
[19] T. Yang, S. Kupershmidt, D.M. Roden, Anti-minK antisense decreases the amplitude of the rapidly activating cardiac delayed rectifier K^+ current, Circ. Res. 77 (1995) 1246–1253.
[20] Y. Yamaguchi, K. Mizumaki, K. Nishida, J. Iwamoto, Y. Nakatani, N. Kataoka, Y. Hata, F. Ichida, N. Nishida, H. Inoue, Abnormal repolarization dynamics during daily life in patients with G38S single nucleotide polymorphism of KCNE1 gene, Heart Rhythm 10 (2012) S212.